PHENOMENOLOGICAL MODELS OF THE 11-YEAR SOLAR CYCLICITY AND ITS EMPIRICAL RULES

Main (Pulkovo) Astronomical Observatory of the Russian Academy of Sciences, St. Petersburg, Russia.

e-mail: vg.ivanov@gaoran.ru

Received February 21, 2025

Revised April 08, 2025

Accepted June 17, 2025

Abstract. The paper describes and analyzes the method of building phenomenological models of the 11-year solar cycle based on the nonlinear oscillator equation with damping and external noise. It is shown that such models are able to reproduce the known empirical relations between the cycle parameters: the Waldmeier and Chernosky rules. The Gnevyshev-Ol rule (in its original "correlation" sense) turned out to be the most difficult to reproduce in the model, and the paper discusses possible ways to overcome this difficulty. It is also noted that the behavior of the constructed models may also include another peculiarity of observational series: long-lasting decreases in the level of global activity ("grand minima").

DOI: 10.31857/S00167940250705e3

1. INTRODUCTION

One of the characteristic manifestations of the nonlinear nature of the 11-year solar cyclicity is the relationships between the amplitude, length, and shape of the cycles. First of all, the anti-correlation between the length of the growth branch of a cycle and its amplitude, the "Waldmeier rule" (WR) [Waldmeier, 1935], is well known. In addition, anti-correlation between the length of a given 11-year cycle from minimum to minimum and the amplitude of the next one ("Chernosky's rule", PC) is noted [Chernosky, 1954; Hathaway et al., 1994; Solanki et al., 2002; Hathaway, 2015; Ivanov, 2021]. There is an indication that the connections described by SP and IF have existed on the Sun for at least half of the last millennium [Usoskin et al., 2021; Ivanov, 2024]. Note that the meaning of these two rules is different: while the SP describes the coupling within a cycle: the dependence of the shape of a single cycle on its amplitude, the IF describes the coupling between neighboring cycles.

The Gnevyshev-Ol rule (GGO) is even more complicated: although it describes the connection between cycles, it does not describe the strength of the connection as such, but its variation: the correlation between the powers of neighboring cycles in a pair is high if the first cycle

in the pair is an even cycle, and much lower if the first cycle is an odd cycle. In addition to this, canonical formulation of the PGO, given in the pioneering paper by Gnevyshev and Ohl [1948], an alternative one, according to which even cycles are followed by higher in amplitude (or more powerful in some other sense) odd cycles, is very often found in publications (see the literature analysis in Nagovitsyn et al., [2024]) , but below we will stick to the canonical (correlation) understanding of this rule.

All these rules are empirical in nature: some correlations are noted in observations, but they have no generally accepted explanation within the framework of consistent physical models of solar cyclicity (e.g., solar dynamo models).

Meanwhile, "phenomenological" models of cyclicity are also of some interest. Such models are built not from first principles, but by selecting a formal mathematical description, in which the behavior of the model, in one sense or another, is similar to its prototype. These models usually do not pretend to a deep physical meaning, but may allow a deeper understanding of some features of the observed phenomena. In relation to solar cyclicity, such an approach was applied, for example, in [Gregg, 1984; Kiselev and Kozlovskij, 1993; Kiselev and Volobuev, 1997; Volobuev, 2006; Aguirre et al., 2008; Spiegel, 2009; Noble and Wheatland, 2011], etc.

In particular, as a criterion of similarity between the observed solar cyclicity and its phenomenological model we can consider the presence of the above-mentioned empirical rules in the dynamics of the model: Waldmeier, Chernosky and Gnevyshev-Ol. In this paper, based on the equation of a nonlinear oscillator with damping and external noise, we construct several variants of the solar cyclicity model and investigate them for the presence of the relationships described by these rules.

2. DATA AND NOTATIONS

As input data, we will use annual averages of the Wolf numbers SN version 2.0 for the years 1700-2023 [Clette et al., 2014] (Fig. 1a). Let us introduce the following notations for the characteristic parameters of 11-year cycles: SN(t) - index value in year t, $t_m(k)$ - year of the minimum of the k-th cycle. where k = -4, -3, ..., 25 is the cycle number according to Zurich numbering, where the 1st cycle started in 1755, $t_{M,0}(k)$ is the year of the maximum of the k-th cycle, $T_{mM,0}(k) = t_{M,0}(k) - t_{m,0}(k)$ is the length of the ascending phase of the cycle, $T_{mm,0}(k) = t_{m,0}(k+1) - t_{m,0}(k)$ - its full length (from minimum to minimum), $SN_M(k)$ - the maximum level of activity in the *k-th* cycle ("cycle amplitude"), $\sum SN(k) = SN(t_m(k)) + SN(t_m(k)+1) + ... + SN(t_m(k+1))$ is the sum of annual averages over the *kth* cycle ("cycle power"). Thus if a cycle number runs over some set of values k_S, we will denote the corresponding set of values of some cycle parameter P by $P(k_S)$.

In a number of average annual indices, the moments of extrema are determined with year precision. We can improve this accuracy by using quadratic interpolation over three index values

near the year of extremum. It is easy to show that the refined moment of minima

$$t_m = t_{m0} + \frac{1}{2} + \frac{SN_{m-1} - SN_{m+1}}{2(SN_{m-1} - 2SN_{m+0} + SN_{m+1})},$$

where SN_{m+j} is the value of the index in year j relative to the minimum. The refined moments of maxima t_M are refined using a similar formula. In what follows we will use these refined values of the extrema, as well as the derived values of T_{mM} and T_{mm}.

2. EMPIRICAL RULES OF THUMB IN THE OBSERVED SN SERIES

In the SN series, the above empirical rules are satisfied with the following linear correlation coefficients r:

1) for SP: $r_{WR} = r(T_{mM}(k), SN_M(k)) = -0.78$, $k = -4, -3, ..., 24$ (Fig. 2a);

2) for IF: $r_{CR} = r(T_{mm}(k_A), SN_M(k_A+1)) = -0.68$, $k_A = -4, -3, ..., 23$ (Figure 2b);

3) for EO: power correlations in even- odd pairs $r_{EO} = r(\sum SN(k_E), \sum SN(k_E + 1)) = +0.91$ ($k_E = -4, -2, 0, 2, 6, ..., 22$, with the "anomalous" pair of cycles 4-5 discarded, Fig. 2c), power correlations in odd-even pairs $r_{OE} = r(\sum SN(k_O), \sum SN(k_O + 1)) = +0.44$ ($k_O = -3, -1, ..., 23$, Fig. 2d), correlation between powers of neighboring cycles without considering parity $r_{AA} = r(\sum SN(k_A), \sum SN(k_A + 1)) = 0.40$.

3. TRANSITION TO THE ALTERNATING SERIES

Since we will study, in particular, the PGO, it is important to distinguish cycles of different parity. For this purpose, it is convenient to use not the original SN index series, but the derived alternating series, which exhibits the 22-year cyclicity corresponding to the magnetic cycle of Hale [Hale, 1913]. The simplest and most common way to do this, dating back to Anderson [1939] and Bracewell [1953], is to assign a plus sign to the indices of cycles of one parity (e.g., odd) and a minus sign to the indices of another (Fig. 1a). However, the obtained curve has characteristic artificial inflection points near minima, which is inconvenient for our purposes. In order to get rid of them, we extract the square root from the values of the SN series before changing the sign [Kozik, 1949]. Then, by changing the signs of even cycles and additionally smoothing the series with a Gaussian filter of width σ = 1y, we obtain a sign-variable series S (Fig. 1b), with which we will work.

4. MODELS "A" AND "AP": EMPIRICAL FUNCTION F

Let us choose as dynamic variables $X = S$ and $Y = dS/dt$. The observed trajectory of the dynamical system in phase space is depicted in Figure 3a. Let us assume that its dynamics is described by a system of two equations

$$\begin{cases} \frac{dX}{dt} = Y \\ \frac{dY}{dt} = F(X, Y) \end{cases}$$

with initial conditions $X(t = 0) = X_0$, $Y(t = 0) = Y_0$. This system is equivalent to one second-order

differential equation describing a nonlinear oscillator of the general form

$$\frac{d^2X}{dt^2} = F\left(X, \frac{dX}{dt}\right). \quad (1)$$

Here F is a function whose values are known to us only at the points of the observed trajectory (where they are equal to dY/dt), and whose form in the whole investigated region of phase space we have to determine. Below it will be convenient for us to use functions of normalized arguments uniquely related to F: $f(x,y) = F(x \cdot X_M, y \cdot Y_M)$, where $X_M = 32$, $Y_M = 12$. The values of x and y in the observed series vary approximately in the range ±1/2. In order to ensure that the solutions are stable, we will need to make assumptions about the behavior of the functions f and F and beyond the boundaries of this range. The simplest (though not the only) way to do this is to supplement the observational data with artificial points corresponding to pairs of potentially "very powerful" cycles, assuming that the latter are similar in shape to the highest pair (18-19) and differ from it only in amplitude (Fig. 3b). By choosing random points on the trajectories of such cycles, we expand the region of space with the given values of F (Fig. 3c). By linearly interpolating these values to a homogeneous lattice with step 1, then smoothing them with a Gaussian filter with σ = 1, we specify the function F_A tabularly, and then its values can be obtained at any point in the region of phase space $|X| \le X_M$ ($x \le 1$), $|Y| \le Y_M$ ($y \le 1$) (Fig. 4) by interpolation. It is more convenient, however, to approximate F_A analytically, using the function $F_{AP}(X,Y) = f_{AP}(X/X_M, Y/Y_M)$. We will use a polynomial regression model for this purpose: by tabulating the function F_A at the nodes of the lattice (X, Y) where $X = -X_M, -X_M + 1, ..., X_M$, $Y = -Y_M, -Y_M + 1, ..., Y_M$, we find the polynomial F_{AP} that minimizes the sum of squares of the differences between F_A and F_{AP} at these nodes. As the tests have shown, in order not to lose the peculiarities of the system dynamics when passing from F_A to F_{AP}, we must take a polynomial of rather high (12th) degree:

$$f_{AP}(x,y) = 0.023 - 2.108x + 0.126y - 1.050x^2 - 0.166xy + 0.886y^2 - 3.040x^3 - 11.179x^2y - 15.524xy^2 + 5.773y^3 + 10.301x^4 - 0.832x^3y - 5.065x^2y^2 - 3.721xy^3 + 2.352y^4 + 0.127x^5 - 16.951x^4y + 65.324x^3y^2 + 45.799x^2y^3 + 19.599xy^4 - 17.822y^5 - 50.240x^6 - 7.978x^5y + 54.197x^4y^2 + 3.177x^3y^3 - 23.846x^2y^4 + 23.985xy^5 - 6.164y^6 + 7.913x^7 + 91.071x^6y - 72.623x^5y^2 - 93.291x^4y^3 - 107.368x^3y^4 - 23.050x^2y^5 - 1.489xy^6 + 22.367y^7 + 104.388x^8 + 41.317x^7y - 123.102x^6y^2 - 41.351x^5y^3 + 23.188x^4y^4 + 13.007x^3y^5 + 25.623x^2y^6 - 46.276xy^7 + 7.171y^8 - 9.260x^9 - 104.001x^8y + 25.616x^7y^2 + 40.162x^6y^3 + 106.168x^5y^4 + 79.284x^4y^5 + 46.576x^3y^6 - 14.143x^2y^7 - 7.584xy^8 - 12.083y^9 - 96.624x^{10} - 50.932x^9y + 104.116x^8y^2 + 45.131x^7y^3 + 31.743x^6y^4 - 11.897x^5y^5 - 61.321x^4y^6 + 14.637x^3y^7 + 3.164x^2y^8 + 29.999xy^9 - 4.535y^{10} + 3.333x^{11} + 37.957x^{10}y - 1.879x^9y^2 + 1.662x^8y^3 - 21.813x^7y^4 - 30.599x^6y^5 - 39.127x^5y^6 - 13.163x^4y^7 + 1.740x^3y^8 + 9.200x^2y^9 + 1.866xy^{10} - 32.476x^{10}y + 2.197y^{11} + 33.051x^{12} + 18.690x^{11}y - 5.435x^9y^3 - 17.258x^8y^4 - 22.378x^7y^5 + 6.074x^6y^6 + 27.267x^5y^7 + 21.905x^4y^8 - 22.279x^3y^9 - 7.332x^2y^{10} - 4.276xy^{11} + 1.197y^{12}.$$

In the ranges X || ≤ X(M), |Y| ≤ Y(M) themodulus of the difference $|F_A(X,Y) - F_{AP}(X,Y)|$ does not exceed 0.23.

Numerical simulations have shown that for both the function $F_{(A)}$ ("model A0") and its approximation $F_{(AP)}$ ("model AP0"), system (1) has a stable limit cycle with a period of about 21 years (Fig. 5a), which corresponds well to the Hale cycle of the observational series. The behavior of the systems described by these two functions is generally similar, although it may differ in minor details, and it is more convenient to use the analytically defined function F_{AP}.

The trajectory of the AP0 model smoothly approaches the limit cycle, which is not similar to the real behavior of solar activity indices. To increase the similarity, we add noise to equation (1) by modifying its right-hand side:

$$\frac{d^2X}{dt^2} = F\left(X, \frac{dX}{dt}\right) + \beta\delta(t) \quad (2)$$

Here δ(*t*) is the "noise function" whose values at moments one year apart are normally distributed random variables with zero mean and unit variance, and its values at intermediate moments are interpolated. Thus, β is a parameter of the model (let's call it "model B") that sets the noise level. Numerical experiments have shown that at β = 0.2, the behavior of the model system is similar to that of the observed system, and we use this noise level hereafter unless otherwise specified. Given a given function *F*, we can vary the initial conditions X_0 and Y_0, as well as the initial state of the noise generator, obtaining different realizations of the AP model. A typical phase trajectory of the system for this model is depicted in Figure 5b.

Using a Monte Carlo approach, we construct a set of 100 random realizations of the AP model with a series of length 500 years (approximately 24 Hale cycles) and obtain estimates of the average SP and IF correlation coefficients and their scatter: r_{WR}= -0.55±0.13, r_{CR}= -0.49±0.14. Both coefficients are somewhat smaller than in the observed series, but are significant at the level of $p \approx 3\text{-}10^{-5}$. As for the EO, its signs do not appear in the model: the correlations of cycle powers in pairs are on average independent of their parity, $r_{EO} \approx r_{OE} \approx 0.8\pm0.1$.

5. MODEL "B": OPTIMIZATION BY LINK STRENGTHS

Thus, by specifying the function *F* describing the dynamics of the system by extrapolating its values at the points of the observed phase space trajectory, we have been able to construct a model in which SP and IF are satisfied, but not PGO.

We can propose an alternative approach to model building: bypassing the extrapolation stage and immediately search for such a function *F* at which the correlations describing the empirical rules are close to their observed values. Suppose that *f(x, y)* is a polynomial of degree 3 without a free term

$$f_B(x,y) = a_1x + a_2y + \ldots + a_9y^3,$$

and we will, varying a_i, minimize the target function

$$H(a_1 1, \ldots, a_1 9) = ((r_1("WR", r) - r_1("WR", m))/r_1("WR", r))^2 + ((r_1("CR", r) - r_1("CR", m))/r_1("CR", r))^2 +$$
$$+ ((r_1("EO", r) - r_1("EO", m))/r_1("EO", r))^2 + ((r_1("OE", r) - r_1("OE", m))/r_1("OE", r))^2 +$$
$$+ ((r_1("AA", r) - r_1("AA", m))/r_1("AA"$$

where $r_{L,r}$ are the correlation coefficients for link L in the observed series, and $r_{L,m}$ are the same in the 500-year realization of the model series constructed using the function f_B. One of the local minima of H corresponds to the function (Fig. 4c)

$$f_B(x,y) = -2.040x + 0.293y + 0.181x^2 - 3.046xy + 1.785y^2 - 0.994x^3 - 8.611x^2y - 7.800xy^2 + 1.840y^3. \quad (3)$$

We will call the models using the found function f_B, "B0" (without noise) and "B" (with noise). Model B0 has a stable limit cycle with length ≈ 23.8y and amplitude $SN_M \approx 190$. A typical realization of model B is shown in Figure 5c, and the relationships between the cycle parameters for this realization are shown in Figure 6. Monte Carlo estimation for 100 realizations shows that the SP, IF, and PGO in model B are performed with correlations r_{WR} = -0.52±0.12, r_{CR} = -0.54±0.12, $r_{(EO)}$= 0.79±0.11 > $r_{(OE)}$ = 0.47±0.19 and r_{AA} = 0.14±0.22 ≈ 0, respectively, which is quite close to the correlations in the observed index. Thus, we have reproduced all three rules of thumb, albeit at the cost of not directly relating the F function to the observations.

It is interesting to understand what causes the asymmetry of pairs of cycles of different parity in model B and its absence in model AP. For this purpose, let us compare typical trajectories of the systems in these models (Fig. 5b and c). Note that in model B the trajectory in the lower half-plane approaches the origin closer than in the upper half-plane, while in the AP model no such asymmetry is observed. Apparently, this is why in the first case a fixed level of random noise leads to a greater loss of information about the state of the system than in the second case, and $r_{EO} > r_{OE}$. For the AP model, this asymmetry of the trajectory is noticeably smaller, so $r_{EO} \approx r_{OE}$.

6. DISCUSSION AND CONCLUSIONS

In summary, we have considered several simple phenomenological models of the 11-year cycle based on the nonlinear oscillator equation with damping and external noise (2). To construct model A and the closely related model AP, we constructed the function F, specifying the nonlinear oscillator return force, based on the dynamics of the observed series. The resulting models describe a system with a cycle of approximately 22-year duration and variable amplitude, in which two rules of thumb are satisfied: Waldmeier and Chernosky, but no signs of the fulfillment of the third rule (Gnevyshev-Ol) are observed.

Note that it is quite easy to construct a model in which the PGO in its alternative sense, as alternation of power cycles of different parity, is fulfilled. For this purpose, it is enough to modify any of the models by adding a constant to the function F in equation (2). From the physical point of

view, such an addition would involve, for example, a permanent dipole magnetic field - e.g., frozen into the radiant zone [Kryvodubskyj, 2006; Karak, 2023]. There have also been successful attempts to build models with such alternation by using delayed coupling between neighboring cycles [Durney, 2000; Charbonneau et al., 2007].

It is more difficult to enforce the PGO in its canonical (correlation) formulation. For this purpose, we proposed a model B in which the function F was purposefully constructed in such a way as to ensure the fulfillment of all three rules. It turns out that for this purpose it is sufficient for the return force to be described by a third degree polynomial (3). In this case, the fulfillment of the CSG is ensured by the fact that the system trajectories on average come closer to zero after odd cycles (at $Y< 0$) than after even cycles (at $Y> 0$), and, in the presence of noise, information about the initial state of the system is lost faster in the first case. However, in the observed index series (Fig. 3a) and in the AP model (Fig. 5b), the trajectory asymmetry with respect to the X axis entailing such an effect is weakly pronounced. This implies that the actual mechanism of PGO formation may not be directly related to how it arises in model B.

So, the A(AP) models have difficulties in reproducing the PGO, despite the fact that the F functions describing the dynamics of these models were constructed on the basis of the behavior of the solar cyclicity, in which this effect is present. Several ways to address this difficulty can be pointed out. First of all, we considered the noise level β in model (2) to be constant, which, generally speaking, does not follow from anywhere. For the occurrence of PGO in the model it would be enough to replace the constant β by a function $\beta(X, Y)$ asymmetric about the *X-axis*. The disadvantage of such a trick is that we are essentially directly introducing into the model the asymmetry we intend to explain. It is also possible that the model we have chosen, described by a second-order differential equation, is too simple for describing the Gnevysheba-Ohl effect.

It is interesting to note that both in the AP model and in the B model the coefficient at the third of degree X, responsible, in the leading approximation, for the symmetric nonlinearity of the return force F, is negative. In the case of the simplest nonlinearities (Duffing oscillator), such a sign of this term corresponds to the rigid characteristics of the amplitude-frequency coupling. Just such a property of the dynamics of the 22-year cyclicity was noted in [Nagovitsyn, 1997; Nagovitsyn and Pevtsov, 2020].

Finally, we note separately that some realizations of the AP and B models are similar to observations in that their behavior is characterized by several cycles of decrease in the global activity level ("grand minima", [Eddy, 1976; Usoskin, 2013]), at which the trajectory "wanders" near the zero of the phase space, and a "quasi-vectorial" peak appears in the power spectrum of the model signal (Fig. 7).

CONFLICT OF INTERESTS

The author declares that he has no conflict of interest.

REFERENCES

1. *Gnevyshev M.N., and Ol A.I.,* On the 22-year cycle of solar activity, Astronomical Journal, 1948, V. 25, No. 1, P. 18-20.
2. *Kozik S.M.,* General view of the eleven-year cycle of the Sun's spot-forming activity, Astronomer. Journal, 1949, V. 26, No. 1, P. 28-37.
3. *Nagovitsyn Yu.A., Osipova A.A., and Ivanov V.G.* The Gnevyshev-Olya rule: modern status, Astronomer. Journal, 2024, V. 101, No. 1, P. 56-64.
4. *Anderson C.N.* A representation of the sunspot-cycle, Terrestrial Magnetism and Atmospheric Electricity, 1939, V. 44, No. 2, P. 175–179.
5. *Aguirre L.A., Letellier C., and Maquet J.,* Forecasting the time series of sunspot numbers, Solar Phys., 2008, vol. 249, pp. 103–120.
6. *Bracewell R.N.,* The Sunspot Number Series, Nature, 1953, V. 171, pp. 649–650.
7. *Charbonneau P., Beaubien G., and St-Jean C.,* Fluctuations in Babcock-Leighton Dynamos. II. Revisiting the Gnevyshev-Ohl Rule, Astrophysic. J., 2007, vol. 658, no. 1, pp. 657–662.
8. *Chernosky E.J.* A relationship between the length and activity of sunspot cycles, Publ. Astron. Soc. Pac., 1954, V. 392, pp. 241–247.
9. *Clette F., Svalgaard L., Vaquero J.M., and Cliver E.W.,* Revisiting the sunspot number: A 400-year perspective on the solar cycle, Space. Sci. Rev., 2014, V. 186, pp. 35–103. https://www.sidc.be/silso/DATA/SN_ms_tot_V2.0.txt
10. *Durney B.R.,* On the difference between odd and even solar cycles, Solar Phys., 2000, vol. 196, pp. 421–426.
11. *Eddy E.A.,* The Maunder Minimum, Science, 1976, vol. 192, no. 4245, pp. 1189–1202.
12. *Gregg D.P.,* A nonlinear solar cycle model with potential for forecasting on a decadal time scale, Solar Phys., 1984, vol. 90, pp. 185–194.
13. *Hale G.E.,* Preliminary Results of an Attempt to Detect the General Magnetic Field of the Sun, Astrophys. J., 1913, vol. 38, pp. 27–98.
14. *Hathaway D.H., Wilson R.M., and Reichmann E.J.,* The shape of the sunspot cycle, Solar Phys., 1994, vol. 151, pp. 177–190.
15. *Hathaway D.H.,* The solar cycle, Living Rev. Solar Phys., 2015, vol. 12, article id. 4.
16. *Ivanov V.G.,* Two Links between Parameters of 11-year Cycle of Solar Activity, Geomagn. Aeron., 2021, vol. 61, no. 7, pp. 1029–1034.
17. *Ivanov V.G.,* The Link between Lengths and Amplitudes of the Eleven-Year Cycle for the

Millennium Sunspot Index Series, Geomagn. Aeron., 2024, vol. 64, no. 7, pp. 1069–1072.

18. *Karak B.B.,* Models for the long-term variations of solar activity, Living Rev. Solar Phys., 2023, vol. 20., article id. 3.
19. *Kiselev B.V., and Kozlovskij A.E.,* The role of external forces in an auto-generation model of solar activity, Geomagn. Aeron., 1993, vol. 33, no. 3, pp. 14–19.
20. *Kiselev B.V., and Volobuev D.M.,* Equation of motion from a geophysical data series, In: 1st International Conference, Control of Oscillations and Chaos Proceedings (Cat. No. 97TH8329), 1997, vol. 2, pp. 246–251.
21. *Kryvodubskyj V.N.,* Amplification of the Steady Toroidal Magnetic Field in Solar Interior and Asymmetry of Sunspot Activity in Neighbouring Cycles. In: Solar and Stellar Activity Cycles, 26th meeting of the IAU, Joint Discussion 8, 17-18 August 2006, Prague, Czech Republic, JD08, id. 19.
22. *Nagovitsyn Yu.A.,* A Nonlinear Mathematical Model for the Solar Cyclicity and Prospects for Reconstructing the Solar Activity in the Past, Astron. Lett., 1997, vol. 23. no. 6. pp. 742–748.
23. *Nagovitsyn Yu.A., and Pevtsov A.A.,* Duffing Oscillator Model of Solar Cycles, Astrophys. J. Lett., 2020, vol. 888, no. 2, article id. L26.
24. *Noble P.L., and Wheatland M.S.,* Modeling the sunspot number distribution with a Fokker–Planck equation, Astrophysic. J., 2011, vol. 732, no. 1, article id. 5.
25. *Solanki S.K., Krivova N.A., Schüssler M., and Fligge M.* Search for a relationship between solar cycle amplitude and length, Astron. Astrophys., 2002, vol. 396, pp. 1029–1035.
26. *Spiegel E.A.,* Chaos and intermittency in the solar cycle, Space Sci. Rev., 2009, vol. 144. pp. 25–51.
27. *Usoskin I.G.,* A History of Solar Activity over Millennia, Living Rev. Solar Phys., 2013, vol. 10., article id. 1.
28. *Usoskin I.G., Solanki S.K., Krivova N.A., Hofer B., Kovaltsov G.A., Wacker L., Brehm N., and Kromer B.* Solar cyclic activity over the last millennium reconstructed from annual ^{14}C data, Astron. Astrophys., 2021, vol. 649, article id. A141.
29. *Volobuev D.,* "TOY" dynamo to describe the long-term solar activity cycles, Solar Phys., 2006, vol. 238, pp. 421–430.
30. *Waldmeier M.,* Neue Eigenschaften der Sonnenfleckenkurve, Astron. Mitt. Eidgenössischen Sternwarte Zürich, 1935, vol. 14, pp. 105–136.

FIGURE CAPTIONS

Fig. 1. a) The SN index (blue) and its cognate variant (red); b) Index $S = \pm SN^{1/2}$.

Fig. 2. Correlation diagrams: a) for the relationship between $T_{mM}(k)$ and $SN_M(k)$ (for SP); b) for the relationship between $T_{mm}(k)$ and $SN_M(k+1)$ (for IF); c) for the relationship between $\sum SN(k)$ and $\sum SN(k+1)$ in even-numbered pairs (for PGO); d) for the same relationship in odd-numbered pairs (for PGO). The red lines are the corresponding linear regressions. The red dot in plot c), which is not involved in the regression construction, corresponds to the pair of cycles 4 and 5.

Fig. 3. a) Trajectory of the observed index S in phase space. The red line is a pair of powerful cycles 18 and 19. b) A pair of cycles 18-19 (red curve) and their artificially stretched amplitude versions (green curves); c) The initial phase space point cloud (blue dots) augmented with artificial cycles (red dots).

Fig. 4. Value maps of the functions $F_A(X,Y)$ (left), its polynomial approximation $F_{AP}(X,Y)$ (center), and the 3rd degree polynomial $F_B(X,Y)$ (right).

Fig. 5. a) Example of the evolution of the AP0 model over 1000 years; b) Example of the evolution of the AP model over 500 years; c) Example of the evolution of the B model over 500 years. In all figures, the cycles on the left are even cycles (S< 0), on the right are odd cycles (S> 0), and the trajectory goes clockwise around the origin.

Fig. 6. The SP (a), IF (b), and PGO (c, d) relationships for model B realizations with Fig. 5c. Correlation coefficients for the links are $r_{WR} = -0.68$, $r_{CR} = -0.71$, $r_{EO} = 0.93$, $r_{OE} = 0.45$. See Fig. 2 for details of the notations.

Fig. 7. a) Example of AP model evolution over 1000 years at $\beta = 0.25$; b) SN model series with "grand minima"; c) Power spectrum of the SN model series.

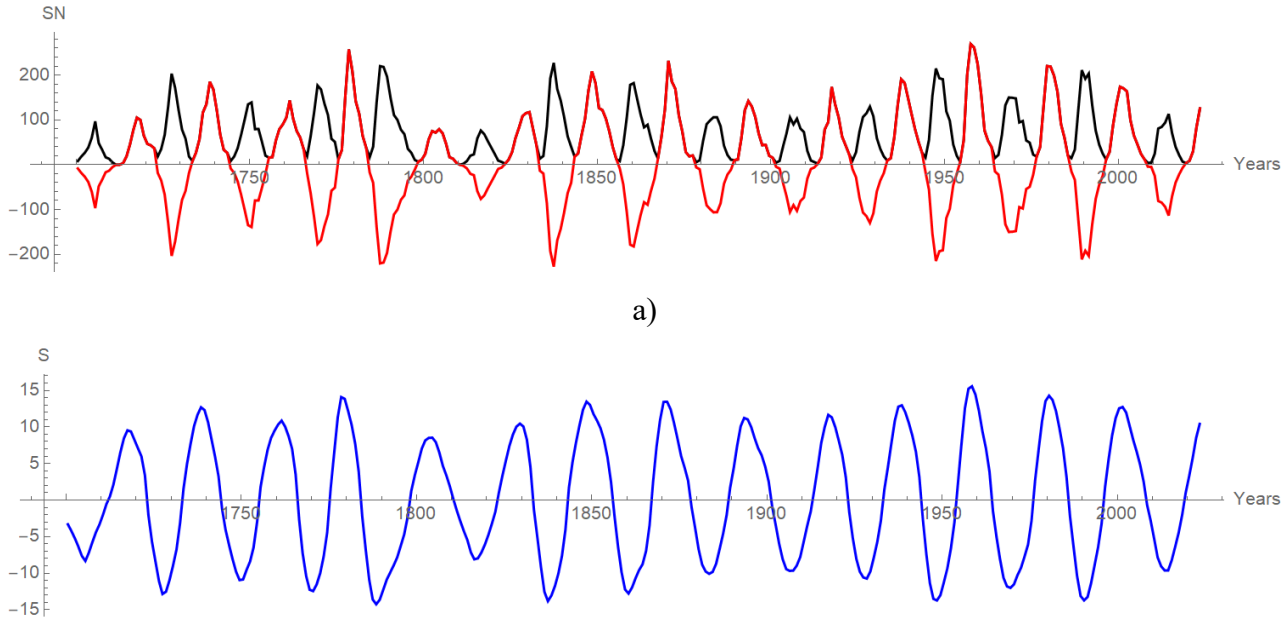
SN
200
100
−100
−200
1750
1800
1850
1900
1950
2000
Years

a)

S
15
10
5
−5
−10
−15
1750
1800
1850
1900
1950
2000
Years

b)

Fig. 1.

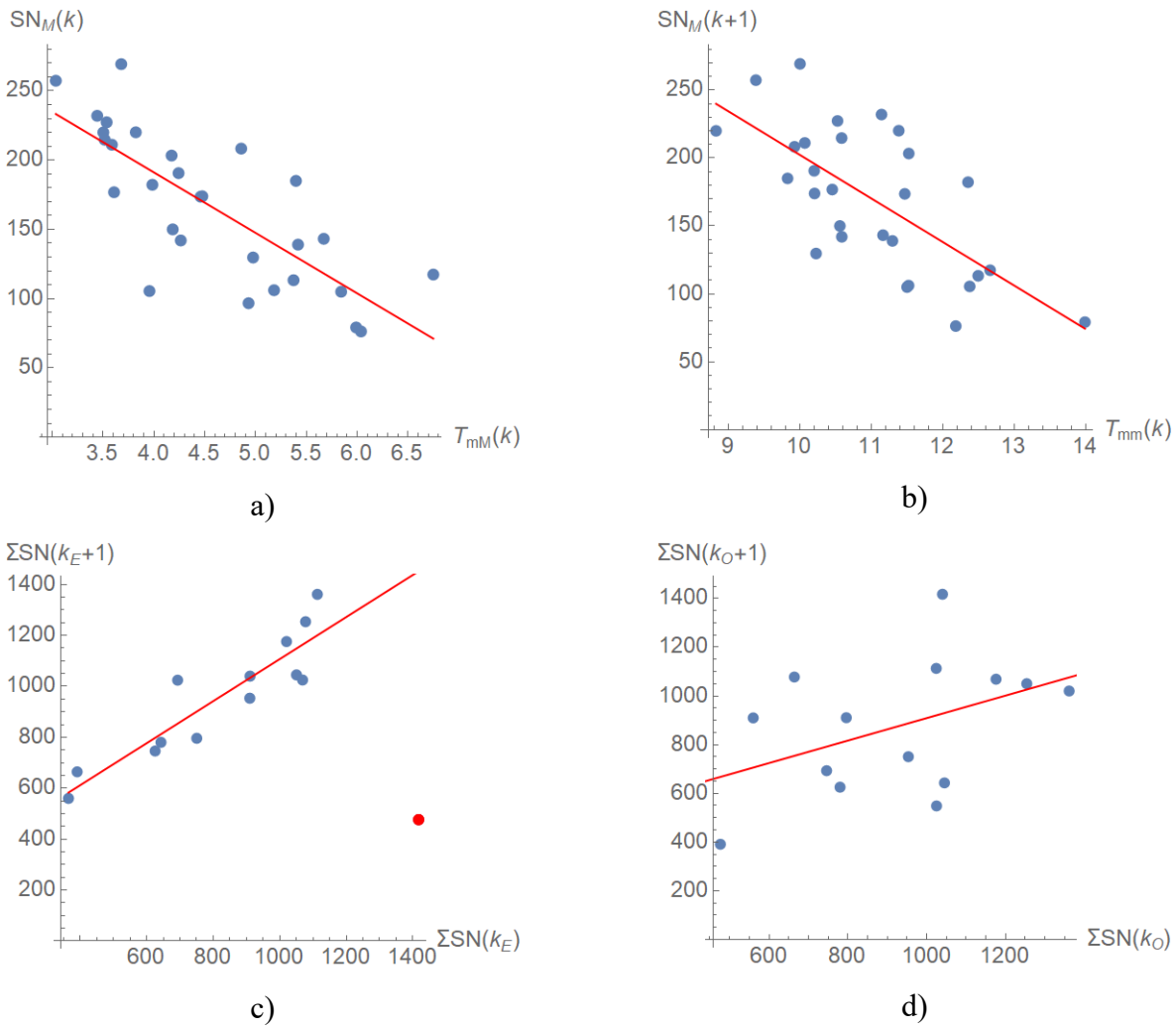
SN_M(k)
250
200
150
100
50
3.5 4.0 4.5 5.0 5.5 6.0 6.5
T_mM(k)
a)
SN_M(k+1)
250
200
150
100
50
9 10 11 12 13 14
T_mm(k)
b)
ΣSN(k_E+1)
1400
1200
1000
800
600
400
200
600 800 1000 1200 1400
ΣSN(k_E)
c)
ΣSN(k_O+1)
1400
1200
1000
800
600
400
200
600 800 1000 1200
ΣSN(k_O)
d)

Fig. 2

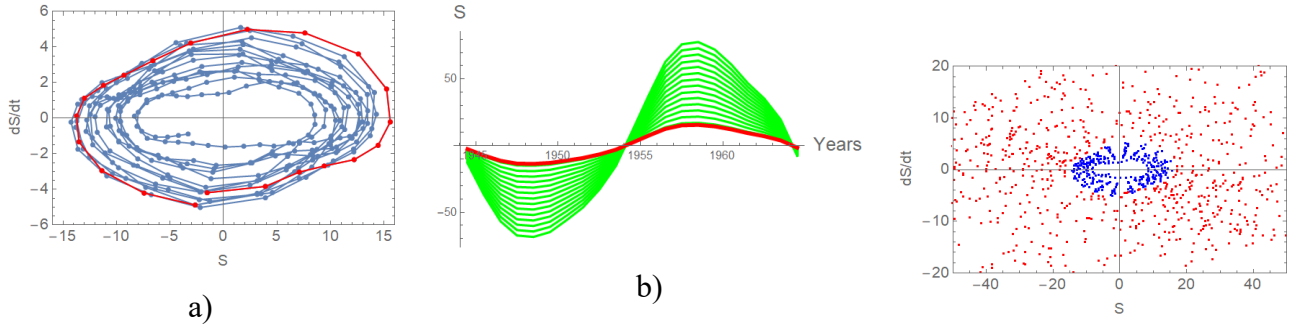

a) b) c)

Fig. 3.

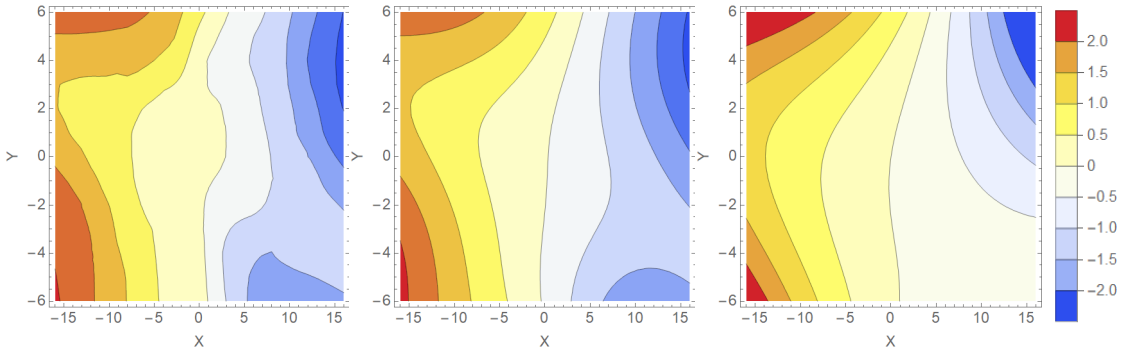

Fig. 4.

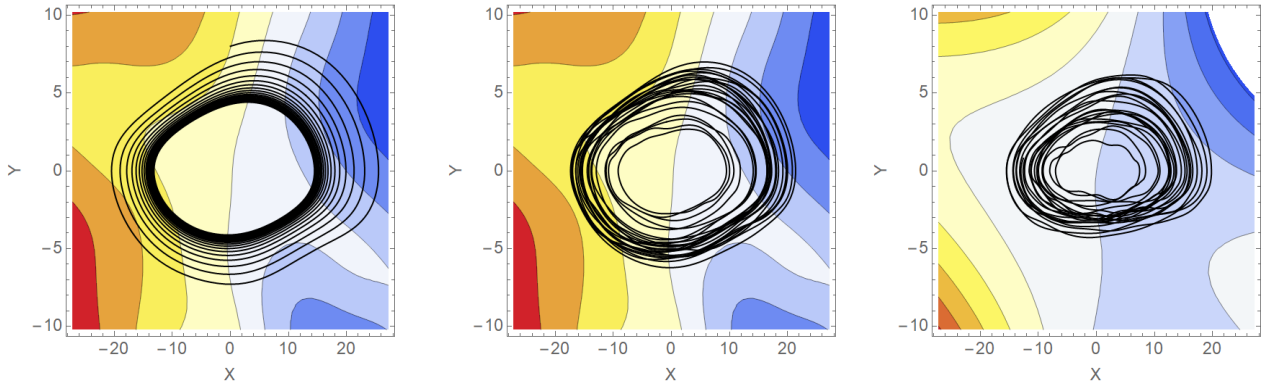

a) b) c)

Fig. 5.

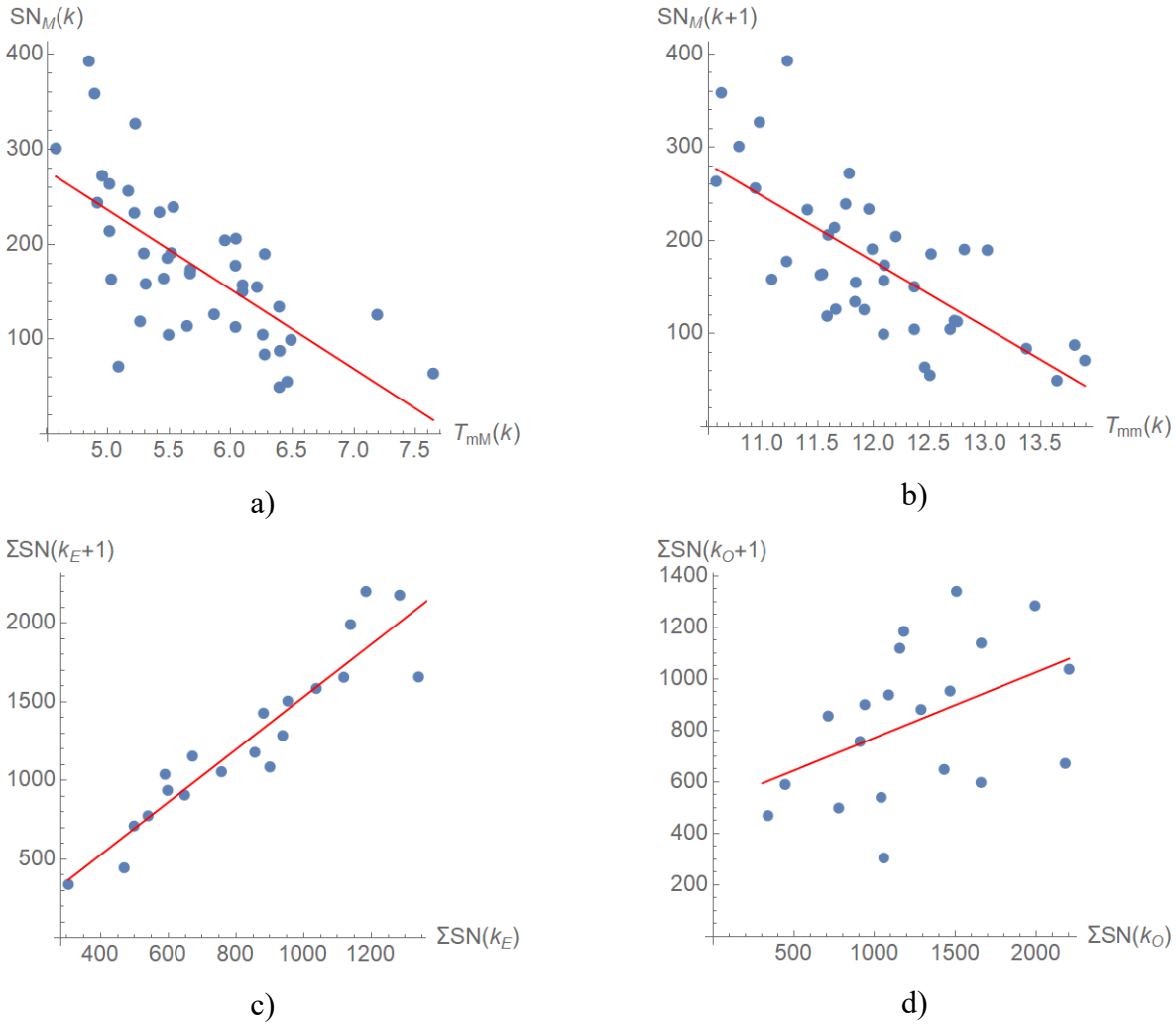
SN$_M$(k)
400
300
200
100
5.0 5.5 6.0 6.5 7.0 7.5
T_{mM}(k)
a)
SN$_M$(k+1)
400
300
200
100
11.0 11.5 12.0 12.5 13.0 13.5
T_{mm}(k)
b)
ΣSN(k_E+1)
2000
1500
1000
500
400 600 800 1000 1200
ΣSN(k_E)
c)
ΣSN(k_O+1)
1400
1200
1000
800
600
400
200
500 1000 1500 2000
ΣSN(k_O)
d)

Fig. 6.

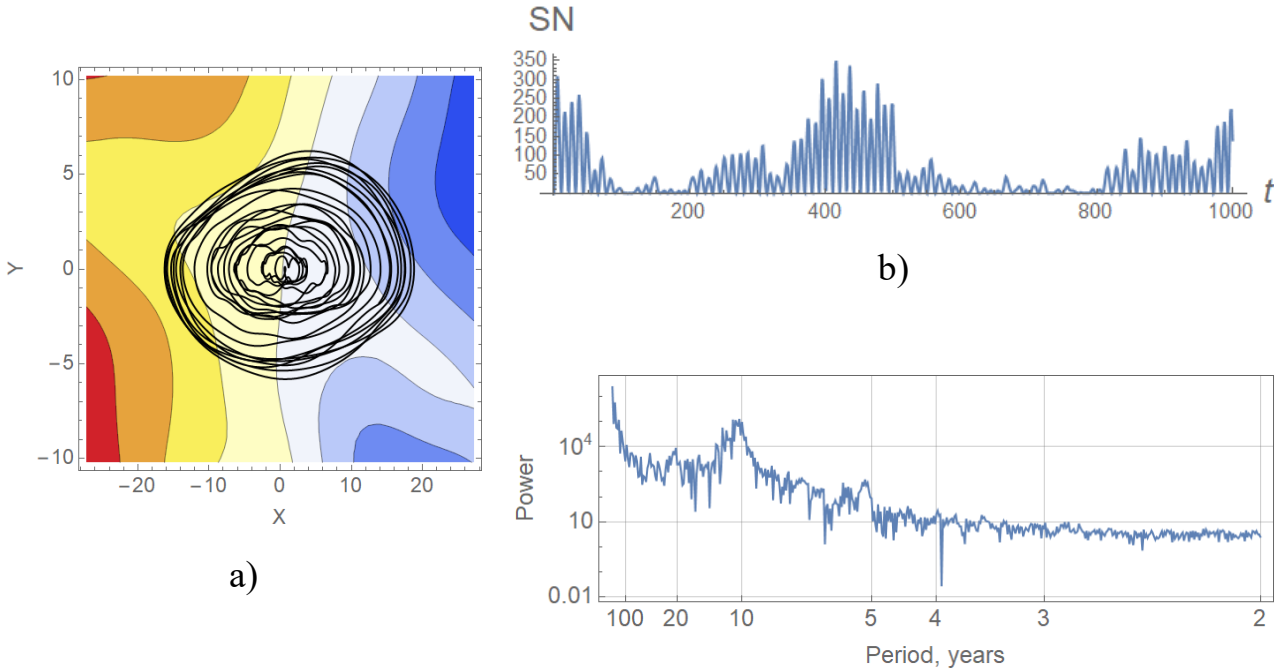
10
5
0
−5
−10
Y
−20
−10
0
10
20
X
SN
350
300
250
200
150
100
50
200
400
600
800
1000
t
Power
10^4
10
0.01
100
20
10
5
4
3
2
Period, years

a)

b)

c)

Fig. 7.